Spectrochimica Acta Part A: Molecular and Biomolecular Spectroscopy 103 (2013) 319–324

Contents lists available at SciVerse ScienceDirect

Spectrochimica Acta Part A: Molecular and Biomolecular Spectroscopy

journal homepage: www.elsevier.com/locate/saa

Structural characterization of N-methylcarbamate: β-Cyclodextrin complexes by experimental methods and molecular dynamics simulations

Natalia L. Pacioni, Adriana B. Pierini, Alicia V. Veglia *

Instituto de Investigaciones en Físico Química de Córdoba (INFIQC), Departamento de Química Orgánica, Facultad de Ciencias Químicas, Universidad Nacional de Córdoba, Ciudad Universitaria, 5000 Córdoba, Argentina

HIGHLIGHTS

- The orientation of N-methylcarbamates in the cavity of β-cyclodextrin is proposed.
- Aromatic vs. alkyl inclusion is determinate from FTIR, DSC, ICD and MD.
- The alkyl rest is included in the case of Promecarb.
- The aromatic interaction is deduced for the others N-methylcarbamates studied.

GRAPHICAL ABSTRACT

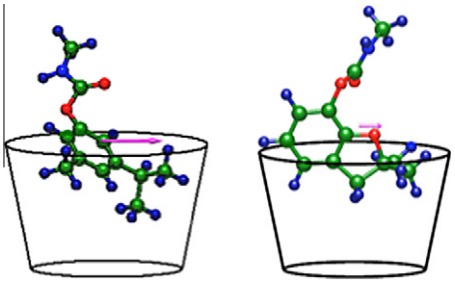

Alkyl vs. aromatic inclusion

ARTICLE INFO

Article history:
Received 6 July 2012
Received in revised form 24 October 2012
Accepted 4 November 2012
Available online 10 November 2012

Keywords:
Inclusion complex
Cyclodextrin
N-methylcarbamates
Insecticides
Complex structure
Inclusion orientation

ABSTRACT

Detailed insights regarding the inclusion process between β-cyclodextrin and the N-methylcarbamates insecticides like Bendiocarb, Carbaryl, Carbofuran and Promecarb, are proposed in bases of experimental and computational methods. The results from Fourier transform infrared spectroscopy, differential scanning calorimetry, induced circular dichroism and molecular dynamics indicate that only in the case of Promecarb the interaction with the macrocycle is produced by the alkyl rest of the molecule. In all other cases the aromatic moiety is the part of the insecticide that is partially included in the cavity of β-cyclodextrin.

Introduction

Research on supramolecular chemistry mainly aims to interpret and design new chemical systems beyond the covalent bond, building on supramolecular structures with specific new properties in molecular recognition, catalysis, separations and sensors, among others [1].

Cyclodextrins (**CD**s) are cyclic oligosaccharides consisting of six (α**CD**), seven (β**CD**) or eight (γ**CD**) units of α-D-glucose linked by α-(1,4) bonds [2]. The shape of the cyclodextrin molecules is that of a hollow truncated cone (a toroid) of height 0.78 nm. These macrocycles can act as hosts (H) to form inclusion complexes with guest molecules (G) both in solution and the solid state. The ability of **CD**s to complex guest molecules into their hydrophobic nanocavity (internal diameter/nm: 0.47–0.53; 0.60–0.65 and 0.75–0.83 for α**CD**, β**CD** and γ**CD**, respectively) [3] has allowed further applications in different fields due to their biocompatibility and the physical chemical changes produced in the substrate included [4]. Therefore, structural characterization of these host–guest complexes is of relevant importance to assist in the correct interpretation of the molecular recognition phenomena, that take

* Corresponding author. Tel.: +54 351 4334170/4334173; fax: +54 351 4333030.
E-mail address: aveglia@fcq.unc.edu.ar (A.V. Veglia).

1386-1425/$ - see front matter © 2012 Elsevier B.V. All rights reserved.
http://dx.doi.org/10.1016/j.saa.2012.11.004

place in these systems, which constitute a fundamental part in the application of cyclodextrin complexes in chemistry, agriculture, foods, cosmetic pharmaceuticals and related technologies [5].

Generally, different techniques have been employed to characterize inclusion complexes either in solution or in solid state. For instance, the interaction between drugs and cyclodextrins in solution has been demonstrated by phase solubility curves [6,7], UV–visible and fluorescence spectroscopy [8], Induced Circular Dichroism (ICD) [6,9], ^{1}H and ^{13}C nuclear magnetic resonance (NMR) [10,11] and microcalorimetry [12], among others. Furthermore, the techniques mostly applied to corroborate the inclusion phenomenon in solid state include the Fourier Transform Infrared Spectroscopy (FTIR) [11,13,14] and Differential Scanning Calorimetry (DSC) [15,16] whereas, the complexes structure, when available, has been determined by X-rays diffraction [17].

Computational methods have also become an important tool to study host–guest systems [5,18]. Ability to predict the main binding modes between a guest and its host through molecular modelling is always a challenge to determine accurately the complexation mechanisms, especially to facilitate the design of new host–guest systems to have desirable properties [19]. Particularly, Molecular Dynamics (MD) simulations allow us to find local and global conformational minima throughout the energy hypersurfaces explored, and distinct from a certain starting geometry [20]. Thus, for the last years MD simulations have been widely used to explore the structural features of **CD**s and cyclodextrin complexes [20,21].

N-methylcarbamate compounds, such as 2,2-dimethyl-1,3-benzodioxol-4-yl methylcarbamate (Bendiocarb, **BC**), 3-isopropyl-5-methylphenyl methylcarbamate (Promecarb, **PC**), 1-naphthylmethylcarbamate (Carbaryl, **CY**) and 2,3-dihydro-2,2-dimethylbenzofuran-7-yl methylcarbamate (Carbofuran, **CF**) (Fig. 1) are widely used as insecticides. We have recently reported the formation of host–guest complexes in water between β**CD** and these N-methylcarbamate insecticides, **CF**, **CY**, **BC** and **PC** with association constants (K_A) values of (190 ± 10) mol^{-1} L^{-1} [22], (330 ± 50) mol^{-1} L^{-1} [22], (510 ± 80) mol^{-1} L^{-1} [23], (1900 ± 200) mol^{-1} L^{-1} [23], respectively, by using UV–visible spectroscopy and fluorescence. Nevertheless, these methods only give a diffuse idea about the complex structure. Although the **CY**:β**CD** complex has been reported in the solid state by DSC and IR and in solution by circular dichroism, no information about the geometrical features of the complex were given [6,7].

In this work, we focus on the structural details of the N-methylcarbamate insecticides:β**CD** complexes in solid state by FT-IR, and for **PC**:β**CD** also by DSC. Furthermore, for the complexes in water, we propose the complexes geometry by interpreting several key clues extracted from the combination of ICD measurements, calculation of the dipolar moment direction for the involved electronic transition, and with molecular dynamics simulations. To the best of our knowledge this characterization has not been reported yet.

We also note that in order to get reliable results by NMR and considering the value of K_A for these pesticides the guest to host ratio (G/H) should be ∼1 with a maxima host concentration in water of ∼10 mM [24]. As water solubility of these insecticides compounds is very low (⩽0.1 mg/mL), NMR measurements were not worthwhile to be done.

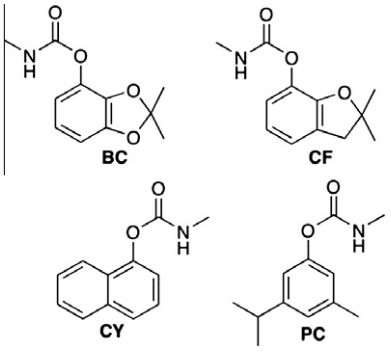

Fig. 1. Structures for the pesticides studied in this work.

Experimental section

Chemicals

Water was obtained from a Millipore apparatus. Bendiocarb (99% purity), Carbaryl (99% purity), Carbofuran (98% purity) and Promecarb (98% purity) (Chem Service); and β-cyclodextrin (Roquette) were used as received. All constituents of the buffers were commercial reagents of analytical grade and were prepared according to literature procedures [25]. The reference buffer solution at pH 7.00 was obtained from monopotassium dihydrogenphosphate (0.02 M); disodium hydrogenphosphate (0.03 M) and sodium chloride (0.02 M).

Preparation of carbamate-β**CD** solid complexes: solid complexes of each of the pesticides mentioned and β**CD** were prepared according to methods described in the literature, with slight modifications [26]. Briefly, 100 mg β**CD** were dissolved in 1.5 mL water at 60 °C assisted by mechanical stirring. After the cyclodextrin was completely dissolved, this was added to the corresponding substrate (equimolar ratio with respect to the cyclodextrin) dissolved in the minimum amount of acetone in an Erlenmeyer. The mixture was stirred at 45 °C for 3 h. Then, the reaction mixture was allowed to reach room temperature and kept protected from light, and stirred for 24 h. The solid obtained was filtered using a nylon membrane (0.2 μm pore size) rinsed with cold water and anhydrous ethyl ether, and then dried under vacuum to constant weight.

Infrared spectroscopy

FTIR spectra (KBr disk) from 4000 cm^{-1} to 400 cm^{-1} were recorded on a Nicolet 5SXC spectrometer applying Fourier transformation of 32 scans, spectral resolution 4 cm^{-1} Analysis of these spectra was done using OMNIC v.5.1 software.

Differential scanning calorimetry

DSC measurements were carried out with a MDSC 2920 TA apparatus. Samples ranging from 1 to 2 mg were placed in pierced aluminum pans and scanned at a rate of 10 °C/min between 50 °C and 200 °C. Dry nitrogen was used as the purge gas (50 mL/min flow rate).

Induced circular dichroism

ICD spectra were collected using a JASCO J-810 spectropolarimeter at 25.0 °C in the range 200–350 nm by taking the average spectrum of five scans on aqueous solutions containing **CY**, **CF**, **BC** or **PC** at a concentration which allowed reaching 0.5 units of absorbance (path length: 2 cm) and 10 mM β**CD**. Each spectrum was corrected by the corresponding blank.

Computational details

All calculations were performed with the Gaussian 03 package. Optimized structures of the substrates were obtained using the

B3LYP hybrid gradient-generalized functional with 6-31G* basis set.

Dipolar moments for the electronic transitions of the substrates were calculated with WinMOPAC version 2.0.2 using INDO/S semiempiric method [27] The σ–σ overlap weighting factor ($OWF_{\sigma-\sigma}$) was 1.267 whereas the $OWF_{\pi-\pi}$ was varied depending on the correlation with experimental results [28], being 0.585 for **CY**; 0.610 for **CF** and 0.629 for **BC** and **PC**. Those transitions, which took place in the range 400–200 nm, were correlated to the UV spectra of each compound.

Molecular Dynamics (MD) simulations were done using AMBER version 7 with GAFF (General Amber Force Field). Atomic charges for all the guest molecules were calculated through RESP fit (restrained electrostatic potential) with HF/6-31G*. The initial structure of the host was taken from CCDC database (Cambridge Crystallographic Data Centre). The pesticide-β**CD** system was surrounded by approximately 9000 molecules of water using the TIP3P model in a periodic box between 15 and 25 Å. No differences in the simulation results were found with the box size. Each MD simulation was run for 3 ns with 2 fs step increments. The system was heated up to 300 K in 0.02 ns, and then it was held at constant temperature (300 K) and 1 atm pressure using the Berendsen method. The equilibration time was 0.5 ns followed by the production step. Through all the simulation, the density fluctuates around 0.99 g/mL. Electrostatic interactions were computed employing the Particle Mesh Ewald (PME) method with 10 Å cut-off for the non-covalent interactions. Non-relevant hydrogen atoms were restricted by SHAKE algorithm. The visualization of the dynamics was done using VMD version 1.8.5, and the variation analysis of RMSd for the host skeleton through the trajectory was determined by ptraj in Amber 7.0.

Results and discussion

Complexes in the solid state

Solid complexes of **CF**, **CY**, **BC** and **PC** with β**CD** were synthesized. In order to characterize their structures, infrared spectra (FT-IR) of the insecticides: β**CD** complexes were analyzed and compared with the spectra of the pure compounds and their physical mixtures (PMs), respectively.

Since the host–guest interactions are non-covalent, the vibrational spectrum of the inclusion compound should not appreciably differ from the spectrum of the corresponding physical mixture [29]. Nevertheless, any significant change in either stretching/bending frequencies (a frequency shift ⩾ instrument resolution, in this case 4 cm^{-1}) and/or intensities confirms the formation of the complex in the solid state [30]. Furthermore, the modification of specific stretching and/or bending group frequencies would indicate that the inclusion within the host cavity is likely to involve that specific group.

Neither of the FTIR spectra (not shown) for the complexes was superimposable with those corresponding to the respective physical mixtures. The main differences observed between the complex and physical mixtures spectra corresponded mainly to band intensities in the 2000–500 cm^{-1} region, belonging to ring vibrations of β**CD** (937–529 cm^{-1}) and/or C═O stretching of the pesticide (1749–1719 cm^{-1}). Particularly the C═O signal showed enhancement of the intensity in the solid complex but no frequency shift, which might indicate that this group is not inside the cavity. Furthermore, disappearance of the signals for water molecules in the cavity (1655 cm^{-1}) was clearly observed for **CY**, **CF** and **BC** complexes, indicating that the pesticides have displaced water molecules from the cavity to form a complex. These differences were attributed to the interaction of the pesticides with the β**CD** cavity in the solid state as was determined previously to occur in solution [22,23]. These results (Tables 1–4) and the assignation of the signals were done according to literature data [13,31]. However, the orientation of the insecticides within the host cavity is not conclusive from these data.

DSC is also a useful technique to confirm inclusion complexes in the solid state. Generally, the interaction of the guest within the cavity of the **CD** modifies its physical properties, such as the melting point [32,33]. For example, the salbutamol:β**CD** complex, in the solid state, did not show the melting point for salbutamol [32]. Similar results have been reported for the prazosine:β**CD** complex [34].

As an additional proof of the formation of the complex in the solid state, we chose to perform DSC measurements of the pesticide with the higher K_A (**PC**, 1900 mol^{-1} M^{-1}), because the stronger the interaction, the larger the modification in the physical properties that we could observe. The DSC scans of the **PC**-β**CD** complex differs from that corresponding to the physical mixture (Fig. 2). The endothermic peak for the melting of **PC** (88.48 °C) showed a slight

Table 1
Selected frequencies of absorption (cm^{-1}) for β**CD** complex with **PC**.

PC		
Frequency (cm^{-1})	Rel. A (complex to PM)[a]	Assignation
1718	1.81	ν**C═O PC**
1250	1.58	ν_{as} C—O—C **PC**
1159	1.55	ν_{as} C—O—C (glycosidic) β**CD**
1027	1.62	Coupled ν**C**—C/ν**C**—O β**CD**
707	1.57	Ring vibration β**CD**
580	1.61	Ring vibration β**CD**

[a] Relative absorption of the band in the complex with respect to the same band in the physical mixture (PM).

Table 2
Selected frequencies of absorption (cm^{-1}) for β**CD** complex with **BC**.

BC		
Frequency (cm^{-1})	Rel. A (complex to PM)[a]	Assignation
1719	1.60	ν**C═O**[b,c] **BC**
1081	0.73	Coupled ν**C**—C/ν**C**—O β**CD**
1029	0.69	Coupled ν**C**—C/ν**C**—O β**CD**

[a] Relative absorption of this band in the complex with respect to the same band in the physical mixture (PM).
[b] In the solid complex, the relative absorption of this band with respect to the signal at 1081 cm^{-1} (coupled ν**C**—C/ν**C**—O β**CD**) is 0.92.
[c] In the physical mixture, the relative absorption of this band with respect to the signal at 1081 cm^{-1} (coupled ν**C**—C/ν**C**—O β**CD**) is 0.42.

Table 3
Selected frequencies of absorption (cm^{-1}) for β**CD** complex with **CY**.

CY		
Frequency (cm^{-1})	Rel. A (complex to PM)[a]	Assignation
1711	3.17	ν**C═O**[b,c] **CY**
1598	3.23	Aromatic ring **CY**
1225	2.21	ν_{as} C—O—C **CY**
1155	1.83	ν_{as} C—O—C (glycosidic) β**CD**
1027	1.79	Coupled ν**C**—C/ν**C**—O β**CD**

[a] Relative absorption of this band in the complex with respect to the same band in the physical mixture (PM).
[b] In the solid complex, the relative absorption of this band with respect to the signal at 1225 cm^{-1} (ν_{as} C—O—C **CY**) is 1.27.
[c] In the physical mixture, the relative absorption of this band with respect to the signal at 1225 cm^{-1} (ν_{as} C—O—C **CY**) is 0.88.

Table 4
Selected frequencies of absorption (cm^{-1}) for β**CD** complex with **CF**.

CF			
Frequency (cm^{-1})	Rel. A (complex)	Rel. A (PM)	Assignation
1709	1.12[a]	0.79[a]	*ν*C═O **CF**
1157	1.61[b]	0.41[b]	ν_{as} C—O—C (glycosidic) β**CD**

[a] Relative absorption of this band with respect to the signal at 1230 cm^{-1} (ν_{as} C—O—C **CF**).
[b] Relative absorption of this band with respect to the signal at 1030 cm^{-1} (Coupled *ν*C—C/*ν*C—O β**CD**).

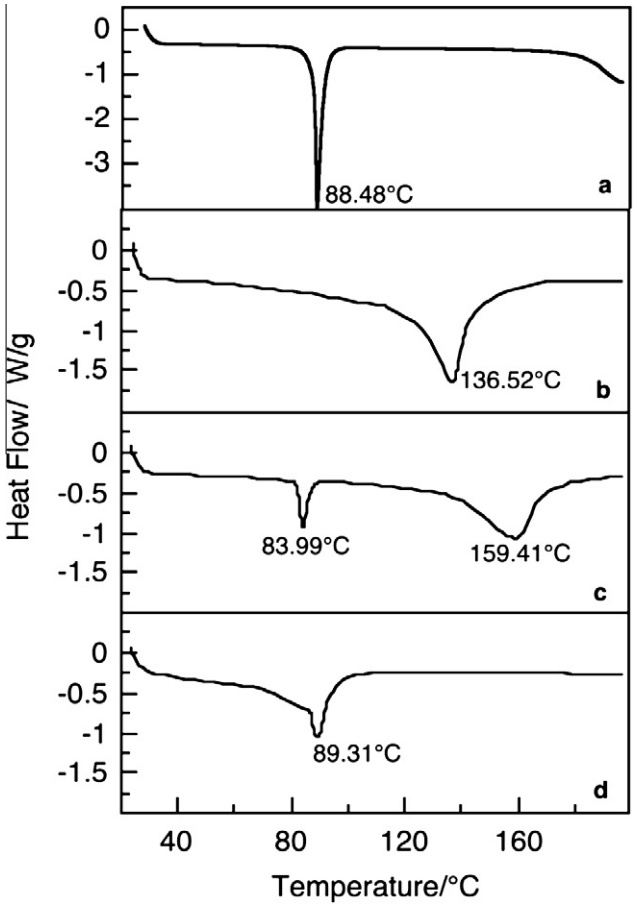

Fig. 2. DSC scans of (a) **PC**, (b) β**CD**, (c) physical mixture and (d) **PC**:β**CD** solid complex.

shift to higher temperatures (89.31 °C) and a decrease in intensity. Moreover, the endothermic peak corresponding to the release of water from the β**CD** cavity was shifted to lower temperatures (shoulder at temperatures lower than 89 °C). This shift to lower temperatures (from 136.52 °C to <89 °C) indicates a weaker interaction between the water molecules contained in the host cavity, as they are displaced by the **PC** inclusion [15]. Interestingly, the shift observed for the endothermic peak of **PC** in the physical mixture (Fig. 2) might indicate an interaction established by the simple mixture of the components.

Structural characterization in solution: induced circular dichroism

General rules for Induced Circular Dichroism (ICD) of a chromophore located inside or outside the cavity of a chiral macrocycle

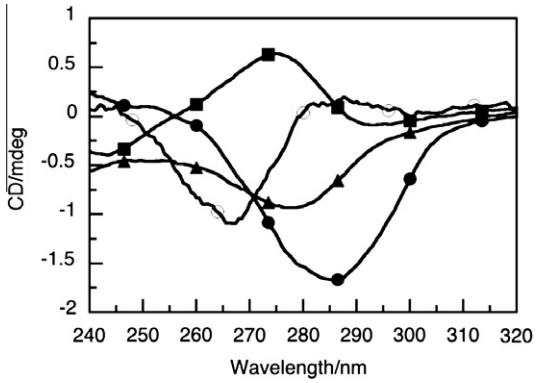

Fig. 3. Induced circular dichroism spectra for insecticides at pH 7.00 in the presence of β**CD**. Curves: (■) [**BC**] = 0.13 mM. (▲) [**CF**] = 0.096 mM. (○) [**PC**] = 0.37 mM and (●) [**CY**] = 0.14 mM. [β**CD**] = 10.0 mM for **BC**, **CF** and **CY**, and 5.0 mM for **PC**.

Table 5
Comparison of experimental data and calculated electronic transition by INDO/S.

Compound	Experimental[a]		INDO/S[b]	
	λ^{max} (nm)	ε (mol^{-1} dm^3 cm^{-1})	λ^{max}	*f*
PC[c]	260	210	260	0.0014
CY[d]	280	4920	279	0.1925
CF[e]	276	2570	275	0.0147
BC[c]	275	1870	274	0.0164

[a] Data correspond to values in water previously reported, Refs. [22,23].
[b] This work.
[c] $OWF_{\pi-\pi}$ = 0.629, Ref. [28].
[d] $OWF_{\pi-\pi}$ = 0.585.
[e] $OWF_{\pi-\pi}$ = 0.610.

have been derived from the Kirkwood–Tinoco equation firstly by Harata and Uedaira [35] and later by Kodaka [36]. These rules have established that when the dipolar moment (μ_{A-B}) for the electronic transition responsible for the absorption of the chromophore (guest), is aligned parallel to the 7-fold symmetry axis of β**CD**, a positive ICD will be observed. On the other hand, if the alignment is perpendicular, the ICD will be negative.

Spectroscopic information obtained from ICD is unique, as the sign and magnitude of the ICD signal depends on the relative orientation of the chromophore within the receptor cavity [37]. ICD as a main tool for determining the orientation of a guest in the cavity of **CD**s has been used with naphthalene derivatives [35,38], substituted benzenes, benzophenone, barbiturics and coumarins [39], methyl phenols [40], indazolinones [9] and bicyclic azoalcanes [41].

From the ICD spectra for **PC**, **CY**, **CF** and **BC** complexes with β**CD** (Fig. 3), the region analyzed corresponds to that where the pesticides absorb (290–250 nm). **BC** showed a positive ICD at 275 nm whereas the other complexes showed negative ICD signals at 286 nm (**CY**), 278 nm (**CF**) and 268 nm (**PC**), indicating that the μ_{A-B} of the **CY**, **CF** and **PC** transitions is aligned perpendicular to the β**CD** axis and parallel for **BC**.

The dipolar moments for the electronic transitions of the different chromophores and the oscillator strength (*f*) were calculated using INDO/S [27] with the optimized geometries of the pesticides. They strongly correlated with experimental data (Table 5).

A default value of 1.267 for the sigma overall weighting factor ($OWF_{\sigma-\sigma}$), as included in the software, was employed; whereas the $OWF_{\pi-\pi}$ was evaluated in order to obtain the best correlation between the experimental absorption spectra and the predicted maximum absorption wavelengths. These $OWF_{\pi-\pi}$ values were in accordance with those reported in literature [28].

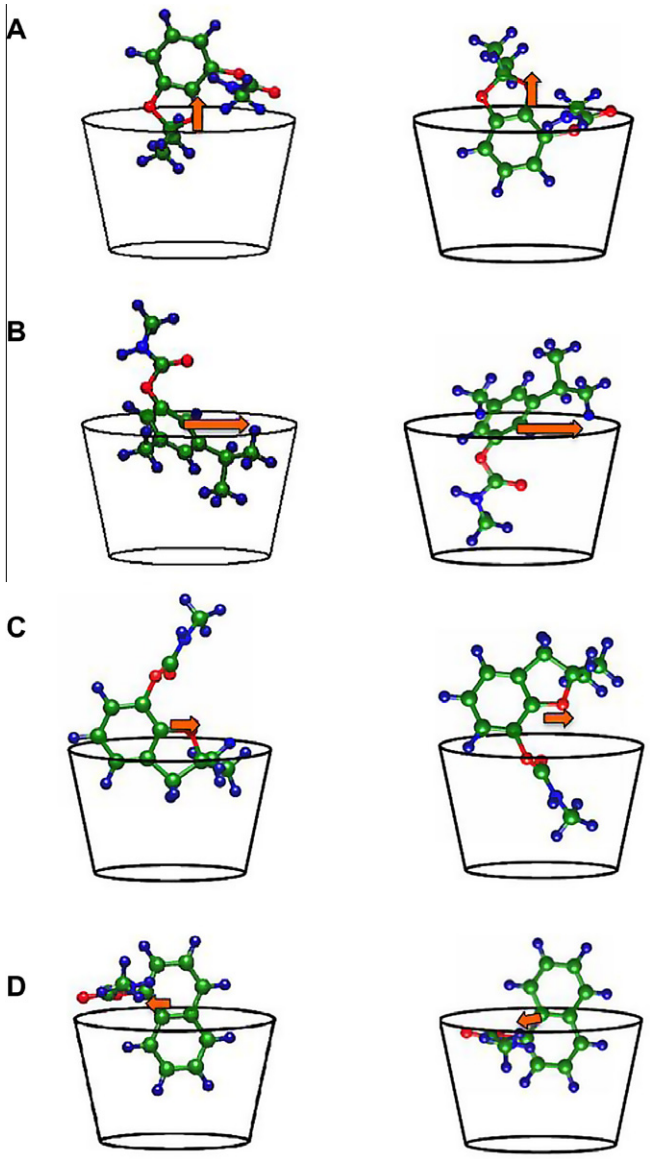

Fig. 4. Possible structures of the different complexes proposed from ICD experiments and INDO/S calculus. The orange arrows indicate the direction of the dipolar moment for the electronic transition calculated by INDO/S. (A) **BC**:β**CD** complex; (B) **PC**:β**CD**; (C) **CF**:β**CD** and (D) **CY**:β**CD**. (For interpretation of the references to color in this figure legend, the reader is referred to the web version of this article.).

From the ICD results and the corresponding calculated μ_{A-B} for the different pesticides, the following illustrations represent the possible complexes geometries (Fig. 4).

Molecular dynamics simulations

Generally, in water, the hydrophobic effect involves the driving force leading to the formation of inclusion complexes between organic molecules with β**CD**. Consequently, it is fundamental to include solvent effects in the calculus of the most stable complex geometries. For this reason, molecular dynamics simulations in explicit solvent were done for the above-mentioned pesticides, with the aim of discerning which of the two probable orientations, determined from ICD and INDO/S data, would be the most favorable.

Molecular Dynamics (MD) simulations were performed starting from both probable orientations (Fig. 4). To gain a greater understanding of the complexation process, the guest was placed in one of the potential orientations but outside the cavity. Interestingly, the complexation took place only for one of the orientations tested, and after 500 ps they were already in equilibrium with a Root-Mean Square Deviation (RMSd) value ⩽2.0. In the case of **PC**, the isopropyl and methyl groups led the inclusion into the cavity (Fig. 4B left). The initial and final structures obtained by MD for PC are shown in Fig. 5. Nevertheless, for **BC** the obtained results did not allow to completely discern between the two possible inclusion modes (Fig. 4A). As regards **CF** and **CY**, the favoured geometries corresponded to those shown in Fig. 4C left and D left, respectively.

Furthermore, in order to compute the interaction energies (Table 6), the four guests were docked to the β**CD** by using

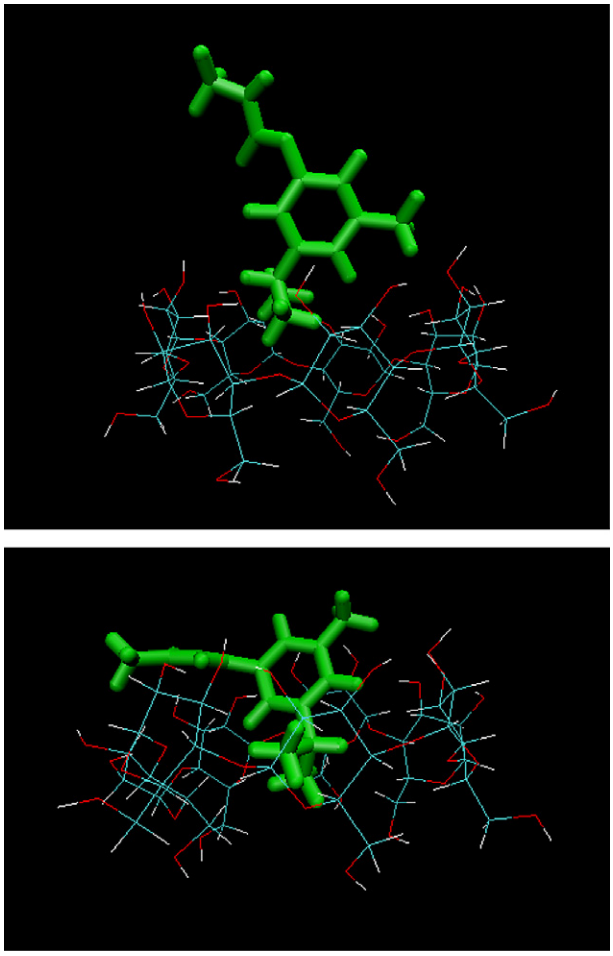

Fig. 5. (Top) Initial structure of **PC**:β**CD** complex before MD. (Bottom) Final geometry of the **PC**:β**CD** complex after 3 ns MD. For simplicity, water molecules are not shown.

Table 6
Energies determined by molecular docking for the preferred orientations.

Complex	ΔG°[a] (kJ mol^{-1})	ΔG°[b] (kJ mol^{-1})
PC:β**CD**	−55.14	−18.70
BC: β**CD**[c]	−38.95	−15.45
BC: β**CD**[d]	−38.74	
CY: β**CD**	−26.07	−14.37
CF: β**CD**	−25.86	−13.00

[a] Determined as the docking energy. Ref. [42].
[b] Determined from the association constant at 298 K. Refs. [22,23].
[c] This complex geometry corresponds to Fig. 4A-left.
[d] This complex geometry corresponds to Fig. 4A-right.

AutoDock [42]. Most stable conformations of the complexes as predicted by docking were in agreement with those obtained as final geometries using MD. It could be noticed that the calculated energies follow the same trend than that of the association constants determined experimentally, although they are systematically lower than the experimental value at 298 K (Table 6). The most stable structure for **CY** is in agreement with similar results reported for other naphthalene derivatives [43]. In the case of **PC**, our results agree with those observed for 3,5-substituted phenols [40] and. For **CF**, the more stable complex geometry found by ICD and MD, in which the benzofuran ring is included, would explain the enhancement of the FTIR signals observed involving the C—O—C strength vibrations (Table 4).

Also, the preferred alkyl vs aromatic inclusion for the N-methylcarbamates studied is in accord with the high vs low value of the association constants determined previously [22,23], as observed for a series of hydroxyphenyl alkyl ketones [44].

Conclusions

Complexes of N-methyl carbamate insecticides and β**CD** are also present in solid state as was confirmed by FT-IR spectroscopy. In solution, the most stable geometries found for the host–guest complexes between β**CD** and N-methylcarbamates were that proposed using ICD combined with INDO/S results, and molecular dynamics simulations.

Acknowledgements

This research was supported in part by Consejo Nacional de Investigaciones Científicas y Técnicas (CONICET), Argentina, Secretaría de Ciencia y Tecnología de la Universidad Nacional de Córdoba (SECyT-UNC) and Agencia Nacional de Promoción Científica y Tecnológica (FONCYT). N.L.P. was a grateful recipient of a fellowship from CONICET. We want to mention the participation of Sebastián J. Castro as training undergraduate student in some determinations of the experimental work.

References

[1] A. Moser, C. Detellier, in: J.L. Atwood, J.W. Steed (Eds.), Encyclopedia of Supramolecular Chemistry, CRC Press, Taylor&Francis Group, New York, 2001, pp. 981–988.
[2] J. Szejtli, Pure Appl. Chem. 76 (2004) 1825.
[3] M.L. Bender, M. Komiyama, Cyclodextrin Chemistry, Springer Verlag, Berlin, 1978;
J. Szejtli, Chem. Rev. 98 (1998) 1743;
J.W. Steed, J.L. Atwood, Supramolecular Chemistry, John Wiley & Sons Ltd., England, 2000.
[4] A.R. Hedges, Chem. Rev. 98 (1998) 2035.
[5] A. Douhal, Cyclodextrin Materials: Photochemistry, Photophysics and Photobiology, Elsevier BV, Amsterdam, 2006.
[6] F. Barbato, M. La Rotonda, A. Miro, P. Morrica, F. Quaglia, J. Incl. Phenom. 38 (2000) 423.
[7] R. Saikosin, T. Limpaseni, P. Pongsawasdi, J. Incl. Phenom. 44 (2002) 191.
[8] R.E. Galian, A.V. Veglia, R.H. de Rossi, Analyst 123 (1998) 1587;
A. Coly, Anal. Chim. Acta. 360 (1998) 129.
[9] M. Kawamura, M. Higashi, J. Incl. Phenom. 51 (2005) 11.
[10] E. Estrada, I. Perdomo-Lopez, J. Torres-Labandeira, J. Org. Chem. 65 (2000) 8510.
[11] S. Cahill, A. Rinzler, F. Owens, S. Bulusu, J. Phys. Chem. 98 (1994) 7095.
[12] V.J. Smith, N.M. Rougier, R.H. de Rossi, M.R. Caira, E.I. Bujan, M.A. Fernandez, S.A. Bourne, Carbohydr. Res. 344 (2009) 2388.
[13] J. Li, D. Yan, X. Jiang, Q. Chen, Polymer 43 (2002) 2625.
[14] O. Dailey Jr., J. Bland, B. Trask-Morrell, J. Agric. Food Chem. 41 (1993) 1767.
[15] J. Villaverde, E. Morillo, J. Perez-Martinez, J. Gines, C. Maqueda, J. Agric. Food Chem. 52 (2004) 864.
[16] J. Gines, M. Arias, J. Perez-Martinez, J. Moyano, E. Morillo, P. Sanchez-Soto, Thermochim. Acta 321 (1998) 53;
T. Van Hees, G. Piel, S. Henry de Hassonville, B. Evrard, L. Delattre, Eur. J. Pharm. Sci. 15 (2002) 347.
[17] K. Harata, J. Chem. Soc. Chem., Commun. (1988) 928;
M. Caira, V. Griffith, L. Nassimbeni, B. van Oudthoorn, J. Incl. Phenom. 17 (1994) 1573;
D. Cruickshank, N.M. Rougier, R.V. Vico, R.H. de Rossi, E.I. Buján, S.A. Bourne, M.R. Caira, Carbohydr. Res. 345 (2010) 141.
[18] K. Lipkowitz, Chem. Rev. 98 (1998) 1829;
E. Castro, D. Barbiric, Chem. Preprint Arch. (2002) 334.
[19] J. Varady, X. Wu, S. Wang, J. Phys. Chem. B. 106 (2002) 4863.
[20] P. Weinzinger, P. Weiss-Greiler, W. Snor, H. Viernstein, P. Wolschann, J. Incl. Phenom. Macro. Chem. 57 (2007) 29.
[21] K.J. Naidoo, J.Y.-J. Chen, J.L.M. Jansson, G. Widmalm, A. Maliniak, J. Phys. Chem. B. 108 (2004) 4236;
R. Consonni, T. Recca, M.A. Dettori, D. Fabbri, G. Delogu, J. Agric. Food Chem. 52 (2004) 1590;
G. Raffaini, F. Ganazzoli, J. Incl. Phenom. Macro. Chem. 57 (2007) 683;
P. Liu, D. Zhang, J. Zhan, J. Phys. Chem. A 114 (2010) 13122;
G. Raffaini, F. Ganazzoli, J. Phys. Chem. B 114 (2010) 7133;
B. Sellner, G. Zifferer, A. Kornherr, D. Krois, U.H. Brinker, J. Phys. Chem. B 112 (2008) 710;
M. Nagaraju, G.N. Sastry, J. Phys. Chem. A 113 (2009) 9533;
L. Lawtrakul, H. Viernstein, P. Wolschann, Int. J. Pharm. 256 (2003) 33.
[22] N.L. Pacioni, A.V. Veglia, Anal. Chim. Acta 488 (2003) 193.
[23] N.L. Pacioni, A.V. Veglia, Anal. Chim. Acta 583 (2007) 63.
[24] K. Hirose, Analytical Methods in Supramolecular Chemistry, C. Schalley/Wiley-VCH Verlag GmbH & Co. KGaA, Weinheim, 2007.
[25] C.R.N. Strauts, J.H. Gilfillan, H.N. Wilson, Analytical Chemistry The Working Tools, vol. I, Oxford University Press, London, 1958. pp. 228.
[26] B. Rao, M. Syamala, N. Turro, V. Rammamurthy, J. Org. Chem. 52 (1987) 5517;
G. Reddy, V. Rammamurthy, J. Org. Chem. 52 (1987) 5521.
[27] W. Anderson, W. Edward, M. Zerner, Inorg. Chem. 25 (1986) 2728.
[28] S. Yuan, Z. Chen, J. Phys. Chem. A 109 (2005) 2582.
[29] S.S. Braga, I.S. Goncalvez, E. Herdtweckb, J.J.C. Teixeira-Dias, New J. Chem. 27 (2003) 597.
[30] L.I. Rossi, R.H. de Rossi, J. Supramol. Chem. 2 (2002) 509.
[31] N. Russell, M. McNamara, J. Incl. Phenom. 7 (1989) 7455;
O. Egyed, Vibrat. Spectrosc. 1 (1990) 225;
K. Nakanishi, P. Solomon, Infrared Absorption Spectroscopy, Holden-Day Inc., USA, 1977.
[32] H. Cabral Marques, J. Hadgraft, I. Kellaway, Int. J. Pharm. 63 (1990) 259.
[33] F. Giordano, C. Novak, J. Moyano, Thermochim. Acta 380 (2001) 123.
[34] L. Liu, S. Zhu, J. Pharm. Biomed. Anal. 40 (2006) 122.
[35] K. Harata, H. Uedaira, Bull. Chem. Soc. Jpn. 48 (1975) 375.
[36] M. Kodaka, J. Phys. Chem. 95 (1991) 2110;
M. Kodaka, J. Am. Chem. Soc. 115 (1993) 3702.
[37] X. Zhang, W. Nau, Angew. Chem. Int. Ed. 39 (2000) 544.
[38] N. Yoshida, H. Yamaguchi, T. Iwao, M. Higashi, J. Chem. Soc. Perkin Trans. 2 (1999) 379;
M. Kodaka, J. Phys. Chem. A 102 (1998) 8101.
[39] N. Berova, K. Nakanishi, R. Woody, Circular Dichroism. Principles and Applications, Wiley-VCH, USA, 2000.
[40] G. Marconi, S. Monti, B. Mayer, G. Kohler, J. Phys. Chem. 99 (1995) 3943.
[41] H. Bakirci, X. Zhang, W. Nau, J. Org. Chem. 70 (2005) 39.
[42] A.J. Olson, P. Graber, M.M. Garrett, D.S. Goddsell, R. Huey, Autodock 3.0., The Scripps Research Institute. Copyright 1999–2001.
[43] I.X. Garcia-Zubiri, G. Gonzalez-Gaitano, J.R. Isasi, J. Incl. Phenom. 57 (2007) 265.
[44] A.V. Veglia, R.H. de Rossi, Can. J. Chem. 78 (2000) 233.